Acoustic properties of auxetic foams

I. Chekkal, C. Remillat & F. Scarpa
Department of Aerospace Engineering, University of Bristol, UK

Abstract

Auxetic foams have raised some interest in noise and vibration control applications as they showed unusual acoustic properties compared to conventional ones, particularly at low frequencies. Auxetic foams are porous materials with a negative Poisson's ratio. They expand in all directions when only pulled in one. In this paper, the acoustic properties of auxetic foams are described both from a numerical and experimental point of view. The acoustic absorption properties of both auxetic and conventional foam samples were measured using a two-microphone impedance tube to provide a comparison between the two types of cellular solids. The acoustical properties of auxetic foams are discussed in terms of the dynamic parameters. A numerical model based on Biot's theory is derived in which the dynamic coefficients of foams are evaluated. Results are compared and commented to provide explanations on the unusual acoustical behaviour of auxetic foams.
Keywords: auxetic foams, dynamic parameters, acoustic properties, porous media, Biot's model.

1 Introduction

Porous materials are commonly used in vibration and noise control applications as they are known for their ability to dissipate acoustic waves propagating in their medium. A porous material consists of a solid phase which is the frame or the skeleton and a fluid phase which is the air or the fluid in pores. Auxetic foams are a subset of porous materials. They can be produced from conventional low density open cell polymer foams by causing the ribs of each cell to permanently protrude inward, resulting in a re-entrant structure. Auxetic foams are characterised by a negative Poisson's ratio. They expand in all directions when only pulled in one. Such unusual behaviour raised some interest in the modern word due to their unconventional mechanical and acoustic properties.


WIT Transactions on The Built Environment, Vol 124, © 2012 WIT Press
www.witpress.com, ISSN 1743-3509 (on-line)
doi:10.2495/HPSM120111

The first auxetic polyurethane PU foam with re-entrant structure was developed by Lakes in 1987 [1]. The re-entrant structure of auxetic foams does not contradict with the classical theory of elasticity since a homogenous isotropic material has a potential Poisson's ratio range between -1.0 and 0.5 [2]. Since then, a wide range of materials featuring the NPR effect has been produced, from long fibre composites to honeycombs and microporous polymers [3].

The wave propagation properties of auxetic materials have been studied from theoretical [4] and numerical/experimental perspectives in composite materials [5] and deterministic cellular structures [6]. In 1994, Howell *et al.* [7] measured the acoustic absorption of NPR foams. Measurements were also carried out by Giffo *et al.* [8] on auxetic foams with small PR values and also doped with MRF (i.e. foam with a magnetorheological (MR) fluid coating) fluid particles [9]. A common characteristic for all the auxetic foams tested was the significant increase in the acoustic absorption at lower frequencies compared to the native conventional foam. However, it is not clear yet how the microstructure of these foams affects their sound properties. In addition, there have been no formal attempts to model the poroelastic parameters of these unusual foams. As a result, the aim of this paper is to evaluate the acoustic properties of open cell auxetic foams by considering a numerical homogenisation to obtain the dynamic poroelastic parameters of Biot's theory [10]. The theory of linear isotropic poroelasticity was first introduced by Biot in 1941 [11]. However, the physical meaning of Biot's parameters is still obscure due to limitations in laboratory measurements of the anisotropic material constants. A homogenization method is applied to the auxetic foam in order to define an approximate mathematical model in which the effective properties of the medium are computed.

2 Experimental testing

In order to study the effect of the manufacturing process on the sound propagation in auxetic foams, normal sound absorption measurements have been performed on conventional and auxetic specimens. The sound absorption properties of auxetic foams were obtained using a two microphone impedance tube following the ISO Standards [12, 13]. The auxetic samples used were produced from conventional open cell PU based foams with 27kg/m^3 density and a 29mm diameter. Results illustrated in Figure 1 show that the manufacturing process applied to conventional foams changes significantly their acoustic properties. The resulting auxetic foams are characterised by a larger absorption in the low frequency range below 1000Hz. At 500 Hz the absorption coefficient of auxetic foams reaches a value of 0.4 compared to 0.3 for their conventional counterpart. At higher frequencies, the absorption coefficient reaches a plateau at 0.8 compared to almost 1 for conventional foams at 1500Hz. The absorption level of auxetic foams remains almost constant within the frequency range 1500–5000Hz. Based on these observations; the aim of this paper is to provide some explanations to the unusual acoustic behaviour of auxetic foams. The dissipation

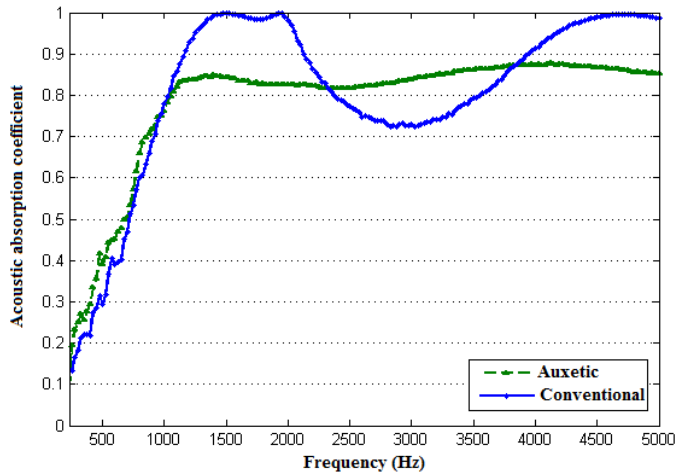

Figure 1: Acoustic absorption coefficient of auxetic and conventional foams.

mechanism is therefore explained in terms of the dynamic parameters of the material.

3 Dynamic poroelastic parameters

3.1 Biot's inertial and viscous coefficients

The finite element analysis developed in this work was mainly based on Biot's theory. Biot's theory describes the propagation of waves through porous media. The assumptions underlying this theory can be found in literature [10, 14]. Biot's constitutive stress strain equations were previously studied by this author to evaluate Biot's Hydrostatic parameters [15]. This paper is then focused on determining Biot's dynamic coefficients, describing the motion of the fluid in the pores. Biot considered a representative elementary volume of the aggregate which is assumed to be small enough compared to the wavelength of the propagating waves. The pore size is assumed to be much smaller than the element being considered. One important result of these assumptions is that the fluid can be considered to be incompressible at the microscopic scale. By assuming a harmonic time dependence of the form $e^{i\omega t}$, the resulting equations of motions are:

$$\begin{aligned} div(\sigma) &= -\omega^2\left(\rho_{11}u + \rho_{12}U\right) + j\omega b(u-U) \\ grad(P) &= -\omega^2\left(\rho_{12}u + \rho_{22}U\right) - j\omega b(u-U) \end{aligned} \tag{1}$$

$$\rho_1 = (1-\phi)\rho_s \qquad \rho_2 = \phi\rho_f \qquad \rho_{12} = -\rho_a \tag{2}$$

$$\rho_{11} = \rho_1 + \rho_a \qquad \rho_{22} = \rho_2 + \rho_a$$

U and u are the average velocities for the fluid and solid phases respectively. σ is the total stress tensor, and P is the pore pressure. Biot's equations of motion are considered to be two coupled vector equations, one representing the average force balance on the solid phase and the other describing the average force balance on the fluid phase. Equation (1) describes the dynamic behaviour of the foam where the term, $j\omega b(u-U)$, is a viscous coupling force proportional to the relative velocity of the two phases. Equation (2) provides expressions for the parameters ρ_{11}, ρ_{12} and ρ_{22} which represent the mass coefficients that account for the effects of momentum transfer between the solid and the fluid phases resulting from the pore tortuosity. ϕ is the porosity, ρ_s is the solid density and ρ_a is the coupling density. Therefore, Biot's dynamic coefficients can be summarised in two important coefficients, the viscous coupling coefficient b and the inertial coupling coefficient ρ_a. Biot showed that at low frequencies, the viscous coefficient b can be written as:

$$b = \frac{\eta}{K_0}\phi^2 \tag{3}$$

η is the viscosity and K_0 is the static permeability. This relation is only valid for low frequency range, where the flow in the foam pores is of a Poiseuille type. For higher frequencies, a correction factor is applied to the viscosity term, replacing it by ηF where F is a complex function of the frequency which is described in section 3.2.

3.2 Modelling Biot's dynamic coefficients

If the porous material is subject to a uniform oscillatory motion, Biot's viscous and inertial coupling coefficients can be evaluated in terms of the resulting oscillatory motion of the fluid. First, the pores are assumed to be cylindrical and the motion of the fluid can be evaluated theoretically by subjecting the wall of the cylinder to a uniform oscillatory motion. In addition to cylindrical pores, conventional honeycomb and re-entrant cell configurations are also considered. It should be noted that the geometric effect of the re-entrant microstructure is an important parameter in which the unusual properties observed in auxetic foams can be explained. Biot defines porous materials as homogenous, two-phase mixture. In this aspect, Biot's model can be considered as a homogenised model of a structure which contains both a fluid phase and a solid phase. Therefore, the approach used in this study is to obtain Biot's parameters using a homogenisation method, for which it is essential to define a representative volume unit. In order to represent the complexity of a conventional and auxetic foam unit cell, 3D honeycomb unit cells were used. A honeycomb cell is a good representation of a conventional porous foam cell, providing the cross-section of a tetrakaidecahedron [16]. Due to the regular geometry of the hexagonal cells used in this study, it is possible to evaluate the overall properties of these cellular structures with analytical solutions [17], or other homogenisation techniques [18]. The foam cells were modelled starting from a parametric template with the

geometric non-dimensional parameters: the wall aspect ratio α (h/l), the relative density β (t/l), and internal cell angle θ (see Figure 2(a)). h and l are respectively the cells horizontal and diagonal rib lengths, and t is the cell's rib density. In the case of re-entrant auxetic cells, a limiting geometric condition was defined by the minimum allowed internal cell angle to avoid the contact of the opposite vertices [19]. In this case, the limiting condition is:

$$\theta_{\lim} = \frac{\pi}{2} - \cos^{-1}\left(\frac{\alpha}{2} - \frac{\beta}{2\sin\varphi}\right) \tag{4}$$

The material skeleton is assumed to be non-deformable because it has a larger density than the fluid. The skeleton is saturated by a Newtonian fluid of viscosity η and density ρ. The sound wavelength is assumed to be much larger than the pore characteristic size, therefore making sure that the fluid can be considered incompressible on the pore scale. It is also assumed that the pressure density variations are decoupled from temperature variations, in other words, thermal effects of the fluid are neglected on any scale. In addition, the fluid phase properties are unaffected at the wall proximity of the solid phase. All pressure gradients and velocity components normal to the boundaries are neglected. The flow direction is assumed to be uniaxial in the z direction which is parallel to the boundaries and the r axis is normal to it where the boundaries are defined by $r = \pm R$ (see Figure 2(b)). The fluid flow equation through a cylindrical pore was previously derived by Biot [10], assuming all quantities are sinusoidal function of time containing the factor $e^{i\omega t}$:

$$\left(\frac{\partial^2 U_f}{\partial r^2} + \frac{1}{r}\frac{\partial U_f}{\partial r}\right) - \frac{i\omega}{\nu}U_f = -\frac{X}{\nu} \tag{5}$$

U_f is the fluid relative velocity, $X\rho = -\frac{\partial p}{\partial x} - \rho\ddot{u}$ and $\nu = \eta/\rho$. Equation (5) is a Bessel differential equation for U_f. It has a general solution which is finite at $r = 0$. For the boundary condition $U_f = 0$ at $r = R$, the following is obtained:

$$\frac{i\omega U_f}{X} = 1 - \frac{J_0\left[i\left(\frac{i\omega}{\nu}\right)^{1/2} r\right]}{J_0\left[i\left(\frac{i\omega}{\nu}\right)^{1/2} R\right]} \tag{6}$$

$J_0\left(i\sqrt{i}z\right) = berz + ibeiz$ with Kelvin functions of the first kind and zero order. To obtain a general solution, the average velocity at the cross section of the tube as well as the friction force at the wall should be determined. The friction force at the wall is $2\pi R\tau$ and the ratio of the friction force to the average velocity can be expressed as follows:

$$\frac{2\pi R\tau}{\langle U_f \rangle} = \frac{2\pi\eta k T(k)}{1 - \frac{2}{ik}T(k)} \tag{7}$$

$T(k) = \frac{ber'k+iber'k}{berk+ibeik}$ Where $k = R\left(\frac{\omega}{v}\right)^{1/2}$, $ber'z = \frac{d}{dz}berz$ and $bei'z = \frac{d}{dz}beiz$. Since the friction force per unit volume of the bulk material in the z direction is:$b\frac{d}{dt}(U_z - u_z)$ and the average flow velocity is $\langle U_f \rangle = \frac{d}{dt}(U_z - u_z)$, the coefficient b is the ratio of the total friction force to the average fluid velocity. For the low frequency limit where $k \to 0$, $b = \frac{2\pi R\tau}{\langle U_f \rangle} \to 8\pi\eta$. At this stage, a correction function $F(k)$ was introduced by Biot to account for the deviation from Poiseuille flow friction as a function of the frequency parameter k. At higher frequencies, the coefficient b is multiplied by a correction factor F(k):

$$F(k) = \frac{1}{4}\frac{kT(k)}{1 - \frac{2}{ik}T(k)} \tag{8}$$

Hovem and Ingram [20] showed that the equations of motions for harmonic excitations can be expressed in terms of the dynamic permeability as well as the frequency correction function F(k). From these equations, they derived an expression for the inertial coupling coefficient $(-\rho_{12})$ as a function of the imaginary part of $F(k)$:

$$(-\rho_{12}) = \left(\frac{\eta}{K_0}\right)\left[\frac{F_i(k)}{\omega}\right] \tag{9}$$

Equations (7) and (9) are used in the evaluation of Biot's dynamic coefficients. Following the analytical method outlined above, numerical models are developed and solved using an embedded software called Comsol Multiphysics with Matlab [21]. The software enables the user to change the cells geometric parameters to account for conventional and auxetic configurations. A set of partial differential equations for the linear incompressible Navier Stokes equations are solved using the finite element discretisation of the problem domain. Each model is subject to appropriate boundary conditions where a linear pressure gradient is applied to the pores. Results are discussed in section 4.

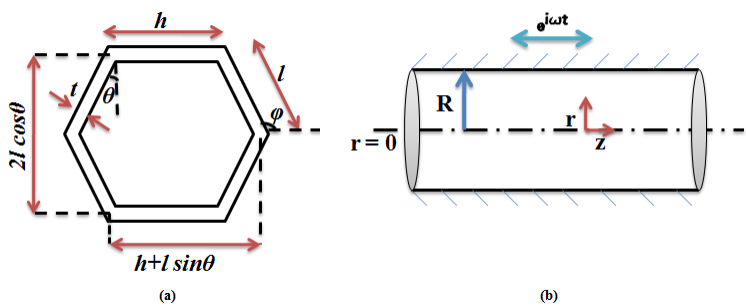

Figure 2: (a) Hexagonal cell geometry and (b) fluid flow model representation.

4 Flow tortuosity and permeability

Applying a macroscopic pressure gradient $\nabla P e^{-i\omega t}$ to an element of a porous medium would result in a linear response of the fluid at the pore scale, i.e. small amplitude variations. The fluid response is defined in terms of the macroscopically averaged fluid velocity$\langle U_f \rangle$. $\langle U_f \rangle$ is therefore linearly related to the applied pressure gradient at any frequency and can be expressed as follows:

$$\alpha(\omega)\rho \frac{d\langle U_f \rangle}{dt} = -\nabla P \tag{10}$$

$$\phi\langle U_f \rangle = -\frac{K(\omega)}{\eta}\nabla P \tag{11}$$

The fluid tortuosity $\alpha(\omega)$ is a dimensionless quantity, independent of frequency as it is a response of an ideal non-viscous fluid [22]. $K(\omega)$ is the frequency dependent permeability and it fulfils the steady state condition where $\omega = 0$. $(-\rho_{12})$ is related to the tortuosity $\alpha(\omega)$ by the following relation:

$$\alpha(\omega) = 1 + \frac{(-\rho_{12})}{\phi\rho} \tag{12}$$

From the finite element analysis of both conventional and auxetic foams, values for the permeability and tortuosity can therefore be evaluated using equations (11) and (12). Results are discussed in the following section.

5 Results and discussion

5.1 Dynamic parameters

Biot's parameters are evaluated numerically and compared to the analytical model. First, the correction function evaluated by Biot is benchmarked against the one calculated in this study using Comsol. The intrinsic values of the model are: $\rho = 1.204\ kg/m^3$, $\eta = 1.846 \times 10^{-5}\ Pa.s$ and R = 500μm. The model was computed for a range of frequencies where $0 < k < 10$. The results obtained from the FEA modelling in this study provide a very good agreement to Biot's evaluation of the frequency correction function (see Figure 3). Low and high limit values for the viscous and inertial coupling coefficients as well as flow permeability and tortuosity have also been benchmarked against analytical limit values in the literature [20, 22]. Results are shown in Table 1. It can be observed that the numerical results of this study match with the analytical solutions. The tortuosity value is slightly higher than the analytical low limit value, however representative to the experimental values of conventional foams.

Further models are developed to investigate the sensitivity of the dynamic parameters to changes in the pore geometry. 3D models of conventional and re-entrant honeycomb structures are computed. Results obtained from all

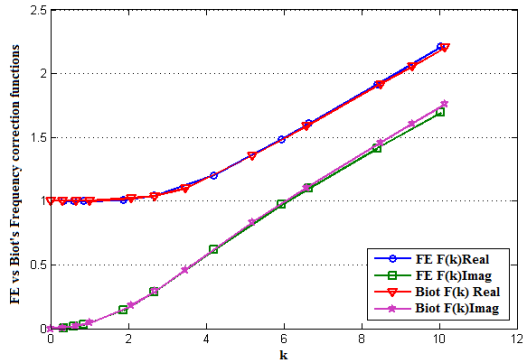

Figure 3: FE and Biot's frequency correction function vs the frequency parameter *k*.

Table 1: Validation results.

	Analytical solutions	Numerical solutions
$b_0 = \lim_{\omega\to 0}(b)$	$8\pi\eta$ = 4.6395*10^-4	4.6396 *10^-4
$\rho_{a0}\ (kg/m^3) = \lim_{\omega\to 0}(-\rho_{12})$	$\frac{\varphi\rho}{3}$ = 0.393	0.4079
$K_0(\mathrm{m}^2) = \lim_{\omega\to 0} K(\omega)$	$\frac{\varphi R^2}{8}$ = 3.0625*10^-8	3.0613*10^-8
$\alpha_\infty = \lim_{\omega\to\infty} \alpha(\omega)$	$\frac{1}{cos^2\theta}$ = 1	1.239

configurations are compared since the volume of all the cells is kept equal. The evaluated dynamic coefficients are plotted against the variation in frequency. As can be seen from Figure 4, values of the Biot's viscous coefficient b increase with increasing frequency for all cell configurations. Values for conventional configurations (i.e. cylindrical and hexagonal pores) are almost equal with changing frequency. Auxetic foams however have higher viscous dissipation compared to conventional ones. On the other hand, the inertial coupling coefficient decreases with increasing frequency. The trend is similar for all cell configurations however; auxetic foams have higher inertial coupling compared to conventional foams. Figure 5 represents the variation of permeability and tortuosity with varying frequency. As expected the permeability decreases with increasing frequency as the fluid flow in the pores becomes more resistant to the dissipation of waves at higher frequencies. At very low frequencies (up to 150Hz), auxetic foams have lower permeability compared to conventional foams, after which the values are closer to those of conventional foams. Moreover, the tortuosity of auxetic foams is higher than that of conventional foams at all frequencies (1.45 for auxetic foams vs 1.35 and 1.34 for conventional foams). This can be explained by the more tortuous path of auxetic foams compared to conventional ones due to their complex microstructure.

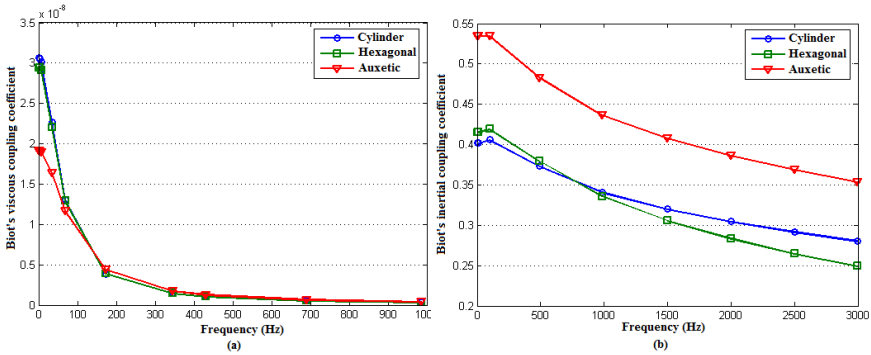

Figure 4: Variation of Biot's (a) viscous and (b) inertial coupling coefficients with frequency.

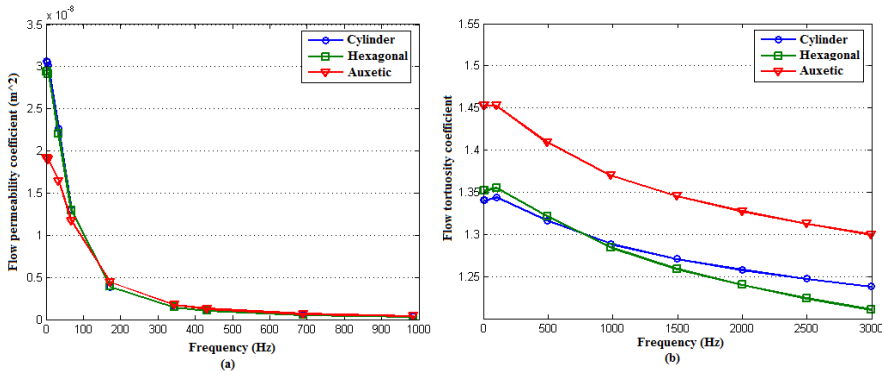

Figure 5: Variation of flow (a) permeability and (b) tortuosity coefficients with frequency.

In addition, the geometry of the hexagonal cell was changed within limitations as a function of the angle theta [20, 25] as expressed in equation (4), while keeping the other geometric parameters h and l, constant. The resulting hydrostatic poroelastic parameters are then plotted against the variation in Poisson's ratio within the range [-0.2, 0.3]. Positive range of Poisson's ratio represents conventional foams while the negative range represents auxetic foams. It can be observed from Figure 6 that the permeability of foams increases with increasing Poisson's ratio. Auxetic foams have lower permeability then conventional ones and values of permeability decrease with the auxeticity of the foams. Furthermore, the tortuosity increases with increasing the auxeticity of the foam. It can also be noticed that the tortuosity values for auxetic foams range between 1.19 and 1.28 whereas they range between 1.19 and 1.21 for conventional foams. Therefore the re-entrant structure of auxetic foam cells has an important effect on the tortuosity of the foam.

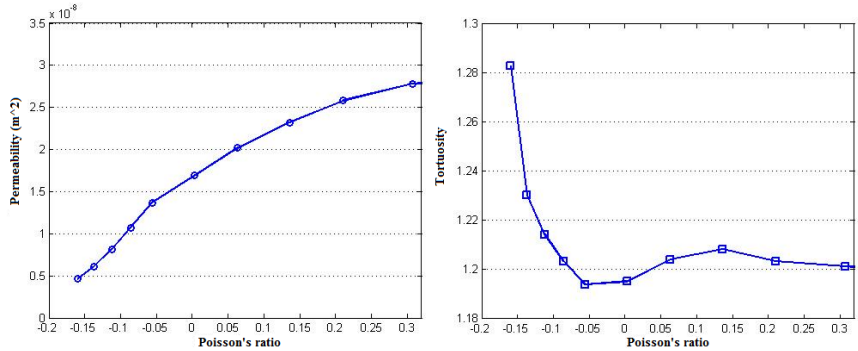

Figure 6: Variation of flow (a) permeability and (b) tortuosity coefficients with Poisson's ratio.

6 Conclusions

In this paper, Biot's dynamic parameters have been successfully evaluated. The numerical models computed showed that auxetic foams have higher viscous dissipation and inertial coupling compared to their conventional counterparts. Due the unconventional microstructure of auxetic foams, the flow becomes more resistant to the dissipation of the sound waves, which explains the higher acoustic absorption at low frequencies and lower sound absorption at higher frequencies. Increasing Poisson's ratio from negative (auxetic) to positive (conventional) values resulted in higher permeability and lower tortuosity. Increasing the auxeticity of the foams results in a more tortuous and more resistant behaviour to the propagation of sound waves.

References

[1] Lakes R. Foam structures with a negative Poisson's ratio. *Science*, 235(4792): 1038–1040, 1987.
[2] Fung Y. C. *Foundations of Solid Mechanics*. Prentice-Hall, 1968.
[3] Yang W., Li Z.-M., Shi W., Xie B.-H., and Yang M.-B. On auxetic materials. *J. Mat. Sci.*, 39: 3269–3274, 2004.
[4] Lipsett A. W. and Beltzer A. I. Reexamination of dynamic problems of elasticity for negative Poisson's ratio. *The Journal of the Acoustical Society of America*, 84(6): 2179–2186, 1988.
[5] Scarpa F. and Malischewsky P. G. Some new considerations concerning the Rayleigh-wave velocity in auxetic materials. *Physica Stat. Solidi B*, 245:578–583, 2008.
[6] Ruzzene M. Spadoni A. and Scarpa F. Dynamic response of chiral truss-core assemblies. *J. Int. Mat. Syst. Struct.*, 17: 941–952, 2006.

[7] Howell B., Prendergast P., and Hansen L. Examination of acoustic behavior of negative Poisson's ratio materials. *Applied Acoustics*, 43(2): 141 – 148, 1994.
[8] Giffo L.G. Scarpa F. and Yates J.R. Dynamic properties of high structural integrity auxetic open cell foam. *Smart Materials and Structures*, 13: 49–56, 2004.
[9] Scarpa F. and Smith F.C. Passive and mr fluid-coated auxetic pu foam - mechanical, acoustic, and electromagnetic properties. *Journal of Intelligent Material Systems and Structures*, 15: 973–979, 2004.
[10] Biot M. A. Theory of propagation of elastic waves in a fluid-saturated porous solid. ii. high-frequency range. *J Acoust Soc Am*, 28:179–191, 1956.
[11] Biot M. A. General theory of three dimensional consolidation. *Journal of Applied Physics*, 12(2): 155–164, Feb 1941.
[12] ISO 10354-2: Acoustics. Determination of sound absorption coefficient and impedance in impedance tubes. part 2: Transfer-function method. In *International Organization for Standardization*, 1998.
[13] ISO 9053: Acoustics. Materials for acoustical applications. determination for airflow resistance. In *International Organization for Standardization*, 1991.
[14] Biot M. A. Theory of propagation of elastic waves in a fluid-saturated porous solid. i. low-frequency range. *The Journal of the Acoustical Society of America*, 28(2):168–178, 1956.
[15] Chekkal I., Bianchi M., Remillat C., Becot F.-X., Jaouen L., and Scarpa F. Vibro-acoustic properties of auxetic open cell foam: Model and experimental results. *Acta Acustica United with Acustica*, 96: 266–274, 2010.
[16] Choi J. B. and Lakes R. Analysis of elastic modulus of conventional foams and re-entrant foam materials with negative Poisson's ratio. *Int. J. Mech. Sci.*, 37:51, 1995.
[17] Gibson L. J. and Ashby M. *Cellular Solids, Structure and Properties*. Cambridge University Press, 1999.
[18] Odegard G.M. Constitutive modeling of piezoelectric polymer composites. *Acta Materialia*, 52(18):5315 – 5330, 2004.
[19] Landi F.P. Scarpa F., Remillat C. and Tomlinson G.R. Damping modelization of auxetic foams. *Smart Structures and Materials*, 3989: 336–343, April 2000.
[20] Hovem J. M. and Ingram G.D. Viscous attenuation of sound in saturated sand. *The Journal of the Acoustical Society of America*, 66(6): 1807–1812, 1979.
[21] Comsol Multiphysics with MatLab. http://www.comsol.com/, April 2011.
[22] Koplik J. Johnson D.L. and Dashin R. Theory of dynamic permeability and tortuosity in fluid-saturated porous media. *J. Fluid Mech*, 176: 379–402, 1987.